

# Determining ammonia emissions from a cattle feedlot with an inverse dispersion technique

T.K. Flesch<sup>a,\*</sup>, J.D. Wilson<sup>a</sup>, L.A. Harper<sup>b</sup>, R.W. Todd<sup>c</sup>, N.A. Cole<sup>c</sup>

<sup>a</sup>Department of Earth and Atmospheric Sciences, University of Alberta, Edmonton, Canada T6G 2E3

<sup>b</sup>Department of Poultry Science, University of Georgia, Athens, GA 30602, USA

<sup>c</sup>Agricultural Research Service, United States Department of Agriculture, Bushland, TX, USA

Received 27 September 2006; received in revised form 5 January 2007; accepted 22 February 2007

## Abstract

An inverse-dispersion technique is used to calculate ammonia (NH<sub>3</sub>) gas emissions from a cattle feedlot. The technique relies on a simple backward Lagrangian stochastic (bLS) dispersion model to relate atmospheric NH<sub>3</sub> concentration to the emission rate  $Q_{\text{bLS}}$ . Because the wind and the source configuration are complicated, the optimal implementation of the technique is unclear. Two categorically different measurement locations (for concentration and winds) are considered: within the feedlot and downwind. The in-feedlot location proved superior, giving a nearly continuous  $Q_{\text{bLS}}$  timeseries. We found average emissions of 0.15 kg NH<sub>3</sub> animal<sup>-1</sup> day<sup>-1</sup> in both 2004 and 2005, representing a loss of 63% (2004) or 65% (2005) of the dietary nitrogen in the animal feed. Downwind measurement locations were less useful for several reasons: a narrow range of useable wind directions; ambiguity in the choice of wind statistics to use in the calculations; low NH<sub>3</sub> concentrations; and downwind deposition of NH<sub>3</sub>. When addressing a large source (like a feedlot) that modifies the ambient wind flow, we recommend in-source measurements for use in inverse-dispersion applications.

© 2007 Elsevier B.V. All rights reserved.

**Keywords:** Trace gas fluxes; Atmospheric dispersion; Atmospheric deposition; Ammonia fluxes; Lagrangian stochastic models; Inverse dispersion

## 1. Introduction

Outdoor feedlots are an important component of beef cattle production in North America. With thousands of animals concentrated in pens, a typical feedlot will be a significant source of trace gases to the atmosphere (e.g., ammonia, methane). Given the impact of these gases, both environmentally and economically, the quantification of feedlot emissions is important.

There are a number of potential methods for measuring feedlot emissions “in situ”. Surface chambers are one possibility (e.g., Boadi et al., 2004). Chambers

enclose a portion of the surface to make a mass balance calculation of emissions, e.g., measuring the flux of gas entering and leaving the chamber, or the gas accumulation rate. While chambers can be simple and inexpensive to use, they have significant disadvantages (Denmead and Raupach, 1993). Because environmental conditions inside a chamber are inevitably altered from ambient, they are no longer truly in situ. Another problem is the small surface area sampled by chambers, typically less than 1 m<sup>2</sup>. Since the horizontal scale of feedlot features (pen dimensions, animal spacing, etc.) is large, multiple chambers are required to get a representative sample of a feedlot. And if cattle or urine spots are direct emission sources, how can these be included?

Micrometeorological techniques overcome some of the limiting disadvantages of chambers. They do not

\* Corresponding author.

E-mail address: [thomas.flesch@ualberta.ca](mailto:thomas.flesch@ualberta.ca) (T.K. Flesch).

alter the surface environment and they typically sample emissions from much larger areas. There are two broad categories of micrometeorological techniques: those measuring the mean *vertical* flux of gas above the surface (e.g., eddy covariance, flux-gradient) or those measuring the *horizontal* flux downwind of the emissions (e.g., integrated horizontal flux). But at a feedlot there may be insufficient “fetch” (upwind distance of feedlot) to apply a vertical flux technique, and/or the feedlot may be too large to use a horizontal flux technique (i.e., measurements required far above ground). The cost and complexity of the necessary sensors (e.g., multiple anemometers, fast response sensors) may also be prohibitive.

A less direct measurement technique is to calculate the mass balance of gas precursors into the feedlot (i.e., feed) and products leaving the feedlot (animals, runoff, manure, etc.). The main difficulty here is measuring all the potential chemical pathways. The studies of Bierman et al. (1999) and Farran et al. (2006) use this laborious technique to estimate ammonia emissions.

In this study we examine a simple and flexible method for measuring emissions. In the “inverse dispersion” technique one models the dispersion of target gas from an emission source to a downwind measurement location. This enables a downwind concentration measurement to establish the emission rate (e.g., Kaharabata et al., 2000; Flesch et al., 2004). This non-interference technique has the advantage of requiring only a single concentration measurement and basic wind information, with substantial freedom to choose convenient measurement locations. The disadvantage is that in its most practical form, the technique entails the assumption of idealized wind conditions, and (within its boundaries) the uniformity of the emission rate. Here we apply the technique to calculate ammonia emissions from a commercial feedlot. The paper has two foci: first the question of the rate of ammonia emission from this feedlot, a question we can answer with reasonable confidence; and second, explore how best to face the ambiguities of the technique, and specifically where best to place sensors in an exercise of this type.

## 2. Inverse dispersion technique

### 2.1. Idealized case

Consider a surface area source located on a simple homogeneous landscape (Fig. 1a), emitting a tracer gas at a uniform but unknown rate  $Q$  ( $\text{g m}^{-2} \text{s}^{-1}$ ). A line-average tracer concentration  $C_L$  ( $\text{g m}^{-3}$ ) is measured in

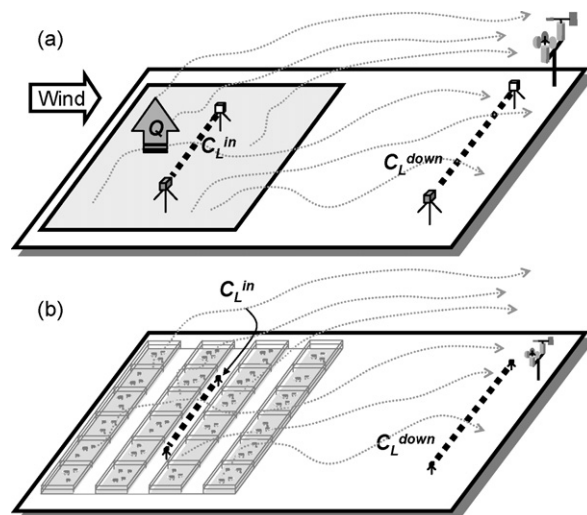


Fig. 1. Using the inverse-dispersion technique to estimate tracer emission rate ( $Q$ ) from two surface area sources: (a) ideally homogeneous source; (b) a cattle feedlot. Line-average tracer concentration ( $C_L$ ) is measured at two alternative locations (inside the source and downwind).

the plume of dispersing gas.<sup>1</sup> With a dispersion model predicting the ratio of the tracer concentration at that location (above background) to the emission rate ( $C_L/Q$ )<sub>sim</sub>, one infers

$$Q = \frac{C_L - C_b}{(C_L/Q)_{\text{sim}}} \quad (1)$$

where  $C_b$  is the background concentration. A number of different dispersion models can provide  $(C_L/Q)_{\text{sim}}$ . Flesch et al. (2004) describe how a Lagrangian (particle tracking) model is well suited for “ideal surface layer problems” like in Fig. 1a. These are environments where Monin–Obukhov similarity theory (MOST) describes the wind near the ground (see Garratt, 1992). In these cases the wind statistics needed to predict  $(C_L/Q)_{\text{sim}}$  can be inferred from the friction velocity  $u_*$ , the Obukhov stability length  $L$ , the surface roughness length  $z_0$ , and the average wind direction  $\beta$ . These primary meteorological properties can be measured or inferred with reasonable ease (e.g., a 3D sonic anemometer).

The hypothetical example in Fig. 1a has other attributes well suited to an inverse-dispersion analysis. The emission source is spatially well defined and homogeneous, there are no other nearby emission

<sup>1</sup> An open-path laser or Fourier transform infrared (FTIR) sensor can give a line-average concentration. A point measurement could also be used, although Flesch and Wilson (2005) argue a line-average provides more accuracy.

sources influencing  $C_L$ , and concentration is measured near the source (i.e., within 1 km). In such an ideal case, Flesch et al. (2004) showed that a timeseries of wind and  $C_L$  observations could be used to calculate average emissions to within 5% of the true value.

## 2.2. Feedlot complications

There are similarities between typical feedlots and our ideal example (Fig. 1a and b). Feedlots are spatially well defined, can be considered nominal surface area sources, and tend to be located in relatively open and homogeneous terrain. But there are important differences. The feedlot surface will undoubtedly be rougher/smooth, moister/drier, warmer/cooler (etc.) than the surrounding terrain. So the layer of air moving over the feedlot undergoes a disturbance whose outcome is the establishment of a new boundary layer in equilibrium with the feedlot surface. Downwind of the feedlot will be another transition, back to the ambient boundary layer. The result is a complex wind environment where the assumptions of MOST do not strictly apply. Furthermore, if we look in detail we find that feedlot emissions are spatially inhomogeneous, with roadways, empty pens, variations in cattle density, etc.

The rigorous approach to dealing with these complexities is to incorporate the correct wind field and source configuration when calculating  $(C_L/Q)_{\text{sim}}$ . Yet measuring or calculating the disturbed wind field is a complex task, and the actual source configuration will generally be unknown. The work of Wilson et al. (2001), Flesch et al. (2005a,b), and McGinn et al. (2006) illustrate that wind and source complexities can often be ignored, and accurate emission measurements made using dispersion calculations that assume ideal winds. The most important factor in such cases is the measurement location for  $C_L$  and the wind ( $u^*$ ,  $z_0$ ,  $L$ ,  $\beta$ ). Fig. 1b illustrates two possible locations: the interior of the feedlot and downwind.

### 2.2.1. In-feedlot measurement

The advantages of an “in-feedlot” measurement location include the likelihood of a relatively high tracer concentration, making for an easier and more accurate measurement compared with downwind. There is also the ability to make emission calculations no matter the wind direction, as the sensors will always be in the emission plume.

A fundamental concern with an in-feedlot measurement is the upwind ambient-to-feedlot wind transition, and how this affects an idealized dispersion calculation. Wilson et al. (2001) studied a similar problem. They

simulated the dispersion of a tracer emitted from a small lagoon, and modeled the wind transition across the upwind land-to-lagoon boundary. The presence of a wind transition makes this lagoon analogous to our feedlot. Wilson et al., found that despite ignoring wind complexity, i.e., using an idealized MOST-based dispersion model to calculate  $(C_L/Q)_{\text{sim}}$ , they could still diagnose lagoon emissions to within 15% of the true value (for a measurement location over the lagoon), except in highly stable stratification.

The accuracy of an idealized calculation should depend on the measurement *fetch* (distance to the upwind surface boundary). As fetch increases we expect less error from ignoring upwind complexity. A traditional scale for evaluating a measurement location is the ratio of measurement height  $z_m$  to the fetch, with smaller values being desirable. In the Wilson et al. (2001) study  $z_m/\text{fetch} = 0.028$ . With the size of typical feedlots (dimensions of hundreds of meters) we anticipate achieving a smaller  $z_m/\text{fetch}$ , and better accuracy than found by Wilson et al.

There is another disadvantage with an in-feedlot location. As argued in Flesch et al. (2005b), the closer a measurement is to the emission source, the more sensitive a dispersion calculation is to the *assumed* source configuration, e.g., the spatial distribution of emissions. Inverse dispersion calculations require a source configuration, yet this is rarely known a priori.

### 2.2.2. Downwind measurement

A downwind measurement location has different advantages: no measurement disruption due to feedlot operations, and reduced sensitivity to the assumed source configuration. Flesch et al. (2005a,b) and McGinn et al. (2006) discuss the advantages of moving downwind of complicated source environments. In these studies the sources (e.g., barns, lagoons) create localized wind disturbances, with a prompt downwind return to ambient conditions. A feedlot creates a different scale of disturbance due to its size. Consider the winds at a measurement location 500 m directly downwind of a 1 km  $\times$  1 km feedlot. For discussion we take a traditional growth rate for boundary layers given by  $z_{\text{SL}}/\text{fetch} = 1/100$  ( $z_{\text{SL}}$  is the height of the new boundary layer at the given fetch). From the ground to a height of 5 m is a wind regime consistent with the ambient landscape downwind of the feedlot. Above this is a remnant regime associated with the feedlot surface. Then even further aloft is a return to the ambient regime attributable to the terrain *upwind* of the feedlot. At this measurement location it is not clear if a single wind observation, from which we extrapolate an idealized

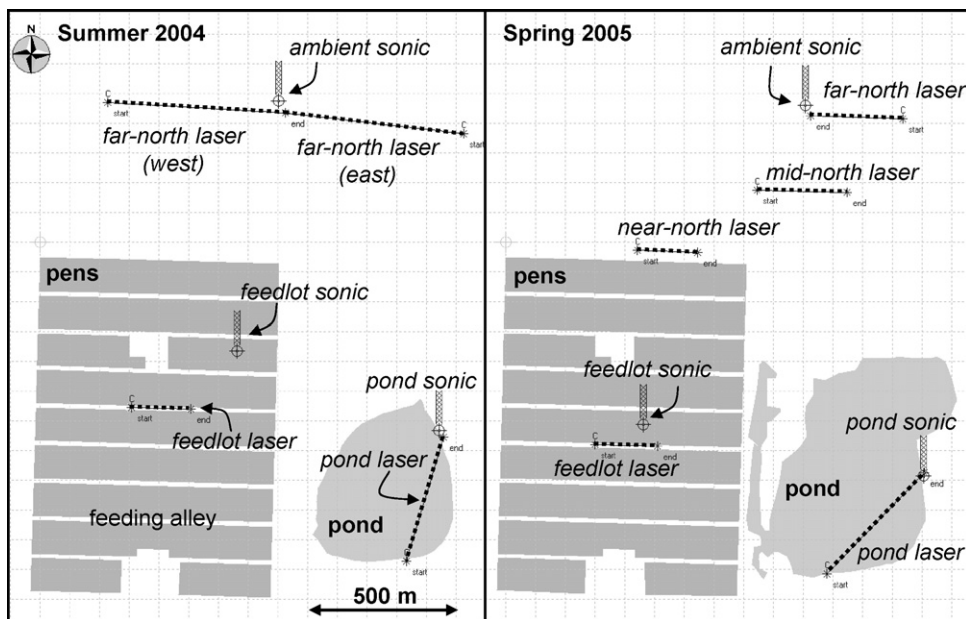


Fig. 2. Feedlot layout in 2004 (left) and 2005 (right). The two far-north lasers in 2004 were treated as a single long-path laser (except when one laser was not functioning). Notice the larger runoff pond in 2005, caused by high precipitation.

MOST wind regime, can adequately represent the winds along the path of dispersing tracers.

Far enough downwind we can imagine a situation where the feedlot wind disturbance has been long “forgotten” by dispersing gases. At this location the ambient winds would sufficiently explain the dispersion of tracer gas, and an idealized dispersion calculation should be accurate. But this distance may be so far downwind as to create other problems: sensitivity to winds above the atmospheric surface layer; likelihood that the feedlot plume misses the measurement location; increasing importance of other transport processes (e.g., deposition); and a concentration rise too small to accurately detect.

### 3. Feedlot experiment

#### 3.1. Site

We measured ammonia emissions from a commercial beef feedlot in Texas (Figs. 2 and 3). The feedlot has a nominal capacity of 50,000 cattle, distributed in hundreds of pens spread over 88 ha (average stocking density of 14 m<sup>2</sup> per animal). Pens are separated by a 1.5 m tall fence (very open, not a windbreak). Within the pen complex are several small buildings, roadways, electrical poles, manure mounds, etc. East of the pens is a large retention pond where runoff is collected. This pond varies in size depending on precipitation. The

surrounding terrain is open and level, having a mix of cropland and pasture. The nearest alternative large ammonia sources are feedlots approximately 10 km distant (west and north).

This semiarid region has hot summers and mild winters. Mean annual precipitation is 500 mm, with 75% falling from April through October. Potential evaporation is about 1500 mm, so that summer precipitation rapidly evaporates. Prevailing winds are southerly to southwesterly (about half the time the wind direction is between 160° and 250°).

#### 3.2. Field measurements

Measurements took place in the summer of 2004 (June) and spring of 2005 (April). Ammonia concentration was measured at several locations using open-path lasers (GasFinders, Boreal Laser Inc., Edmonton, Canada).<sup>2</sup> These gave the line-average concentration between the laser and a retro-reflector (separated by 200–600 m). Laser signals were processed to give 15-min average concentrations ( $C_L$ ). Reported mixing-ratio concentrations (ppm<sub>v</sub>) were converted to absolute concentration (g m<sup>-3</sup>) using the average air temperature

<sup>2</sup> Listing of source names does not imply endorsement or preferential treatment by the University of Alberta, University of Georgia, or the United States Department of Agriculture.

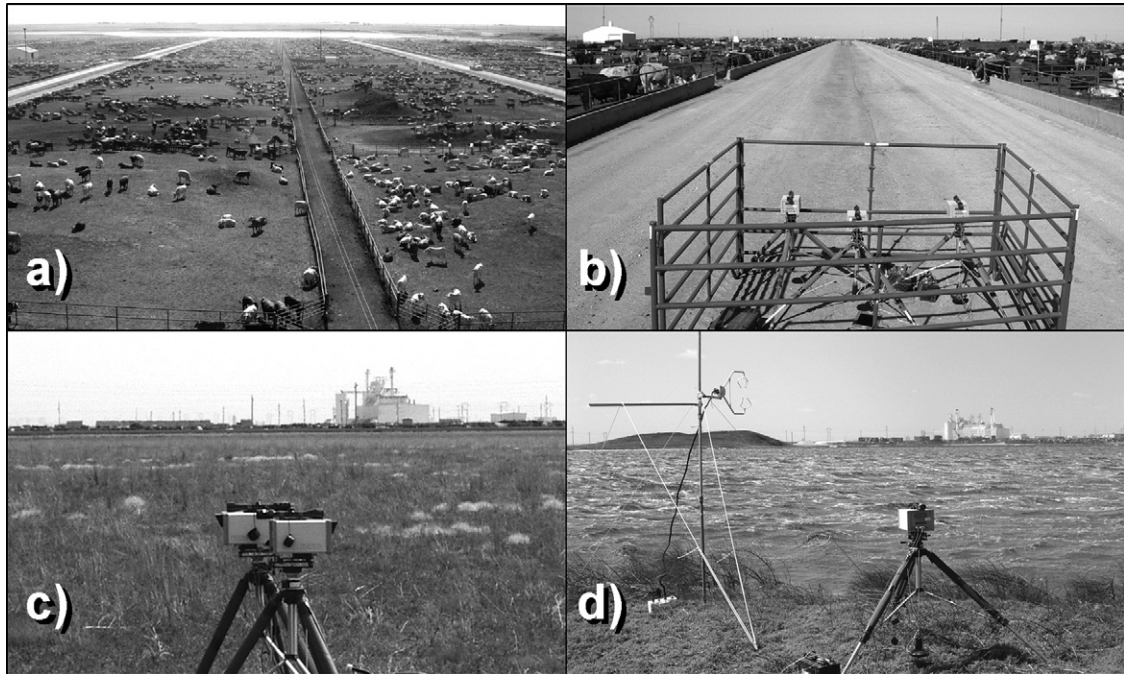


Fig. 3. Photographs of: (a) feedlot pens with runoff pond in far background; (b) in-feedlot lasers; (c) far-north laser units with feedlot in background (2004); (d) pond laser and sonic anemometer (2005).

and assuming an atmospheric pressure of 880 hPa (based on elevation). Lasers were calibrated on-site before each observation period, using a calibration tube flooded with a gas standard.

The feedlot wind environment is described by simple MOST relationships defined by  $u_*$ ,  $L$ ,  $z_0$ , and  $\beta$ , as provided by three-dimensional sonic anemometers (CSAT-3, Campbell Sci., Logan, UT).<sup>3</sup> For each 15-min observation we calculated an average wind direction  $\beta$ , and then transformed the velocity and heat flux statistics into along/across wind coordinates using two coordinate rotations (yaw and pitch corrections, e.g., Kaimal and Finnigan, 1994), with

$$u_* = \sqrt[4]{\langle u'w' \rangle^2 + \langle v'w' \rangle^2}, \quad L = -\frac{u_*^3 T}{k_v g \langle w'T' \rangle},$$

$$z_0 = \frac{z_{\text{son}}}{\exp(Uk_v/u_* - \varphi)}$$

where  $\langle u'w' \rangle$  and  $\langle v'w' \rangle$  are velocity fluctuation covariances (see Garratt, 1992),  $T$  is the average acoustic air

<sup>3</sup> One could argue that cattle give a rough surface whose wind profile is more accurately described by adding a “zero-plane displacement”  $d$  (Garratt, 1992). We believe there is little advantage to adding this problematic parameter (how would  $d$  be measured? how would we generalize winds below  $d$ ?) given the relatively low and uneven density of moving cattle.

temperature from the sonic<sup>4</sup> ( $K$ ),  $k_v$  is von Karman’s constant (0.4),  $g$  the gravitational constant,  $\langle w'T' \rangle$  the vertical kinematic sensible heat flux,  $z_{\text{son}}$  the height of the sonic,  $U$  the average alongwind velocity at  $z_{\text{son}}$ , and  $\varphi$  is a stability correction (we used formulae given by Paulson, 1970; Dyer, 1974). The anemometers also provided velocity standard deviations ( $\sigma_{u,v,w}$ ) used in our dispersion calculations.

Sensor positions are shown in Fig. 2. In both study periods an  $\text{NH}_3$  concentration was measured along a feeding alley near the center of the feedlot (Fig. 3b), at a height  $z_m = 1.2$  or  $1.0$  m. A “feedlot sonic” anemometer was placed above an empty pen at height  $z_{\text{son}} = 7$  m. Two or three lasers were located in the unoccupied pasture north of the feedlot (Fig. 3c) in anticipation of southerly winds ( $z_m = 1.2$  or  $1.75$  m). An “ambient sonic” was placed in the north pasture approximately 600 m from the feedlot with  $z_{\text{son}} = 2.1$  m. We also measured  $C_L$  over the retention pond (to quantify pond emissions), and a “pond sonic” was placed at the pond edge (Fig. 3d).

<sup>4</sup> Kaimal and Gaynor (1991) argue that acoustic temperature can be used when computing  $L$ .

### 3.3. bLS calculations

A bLS dispersion model was used to calculate  $(C_L/Q)_{\text{sim}}$  for each 15-min observation. We used the software “WindTrax” (Thunder Beach Scientific, Nanaimo, Canada), which combines the bLS model described by Flesch et al. (2004) with an interface where sources and sensors are mapped. In the bLS model thousands of trajectories are calculated *upwind* of the laser path for the prevailing wind conditions. The important information is contained in the trajectory intersections with ground (“touchdowns”) and one computes

$$\left(\frac{C_L}{Q}\right)_{\text{sim}} = \frac{1}{N} \sum \left| \frac{2}{w_0} \right|$$

where  $N$  is the number of computed trajectories,  $w_0$  the vertical velocity at touchdown, and the summation covers only touchdowns within the source.<sup>5</sup> The touchdowns map the concentration “footprint”, i.e., the ground area where emissions influence concentration (see Fig. 4).

The site was mapped with a GPS system, and the feedlot represented as a collection of homogeneous area sources (details discussed in Section 5.2). We calculated  $(C_L/Q)_{\text{sim}}$  using  $N = 60,000$  to  $1,000,000$  trajectories. The value of  $N$  was chosen to keep the stochastic uncertainty in  $Q_{\text{bLS}}$  suitably small (i.e., to keep the standard deviation in  $Q_{\text{bLS}}$ , given by 10 subgroups, to less than approximately 10% of the average). Background  $\text{NH}_3$  was assumed to be  $C_b = 0.015 \text{ ppm}_v$ , determined when lasers measured “fresh-air” outside the feedlot.

Not all observations permit good emission estimates and we followed the selection process of Flesch et al. (2005b). Three criteria were used to remove periods of potential MOST inaccuracy:

1. Removed periods where  $u_* \leq 0.15 \text{ m s}^{-1}$  (low wind conditions),
2. where  $|L| \leq 10 \text{ m}$  (strongly stable/unstable atmosphere),
3. where  $z_0 \geq 1 \text{ m}$  (associated with errors in wind profile).

For some wind directions the feedlot plume only “glanced” the path of the north lasers (Fig. 4c). This caused three problems. First, the plume edge carries

greater  $(C_L/Q)_{\text{sim}}$  uncertainty, since extreme trajectories at the plume margin are less predictable. Second, because the edge of the plume is associated with emissions at the feedlot edge, such periods can give a poor estimate of the overall emissions. And third, with only the edge of the plume in the laser path, slight errors in the wind observations (particularly wind direction) can introduce dramatic errors in  $(C_L/Q)_{\text{sim}}$ . To avoid these problems we:

4. Removed periods where the north laser touchdown field covered less than 10% of the pen area (Fig. 4c).<sup>6</sup>

When analyzing the in-feedlot measurements, we ignored periods where the touchdown field covered less than 5% of the pen area (Fig. 4f), to avoid unrepresentative estimates.

## 4. Retention pond emissions

The possibility that the retention pond is a significant source of ammonia, in addition to the pens, is a concern for our analysis. Having strong adjacent sources would mean many of our observations are in a blended emission plume, confounding a  $Q$  inference. We suspected the pond was the much smaller emission source. To confirm this we placed a laser and sonic anemometer at the eastern edge of the pond (Fig. 2) and calculated pond emissions ( $Q_{\text{pond}}$ ) with the bLS approach. This is done for a narrow range of southwest winds, when the pond laser “sees” only emissions from the pond, and the sonic measures the properties of the pond boundary layer. This is a configuration analogous to the lagoon studied by Wilson et al. (2001). Unfortunately, the restrictions on wind direction make for a sparse record of  $Q_{\text{pond}}$  (Fig. 5).

In 2004 the total pond emissions ranged from 2 to 12  $\text{kg NH}_3 \text{ h}^{-1}$ , with an average of  $170 \text{ kg day}^{-1}$  (data not evenly distributed over the day). In 2005 the emissions varied from 6 to 41  $\text{kg h}^{-1}$ , with an average of  $274 \text{ kg day}^{-1}$ . The larger emissions in 2005 correspond to a larger pond: on a per-area basis we see similar emissions of  $9 \text{ kg ha}^{-1} \text{ day}^{-1}$  (2004) and  $8 \text{ kg ha}^{-1} \text{ day}^{-1}$  (2005). The dominant relationship we observe is between the wind and emissions. Fig. 5 indicates a linear relationship between  $Q_{\text{pond}}$  and the friction velocity  $u_*$ , particularly in 2005. A

<sup>5</sup> The units of  $Q$  are  $\text{g m}^{-2} \text{ s}^{-1}$  in this equation. Hereafter we multiply the areal emission rate by the source area and report  $Q$  as an area-integrated emission rate with units of  $\text{kg h}^{-1}$ .

<sup>6</sup> WindTrax calculates the fraction of source pixels displayed as touchdowns on the computer screen. This provides our estimate of touchdown coverage.

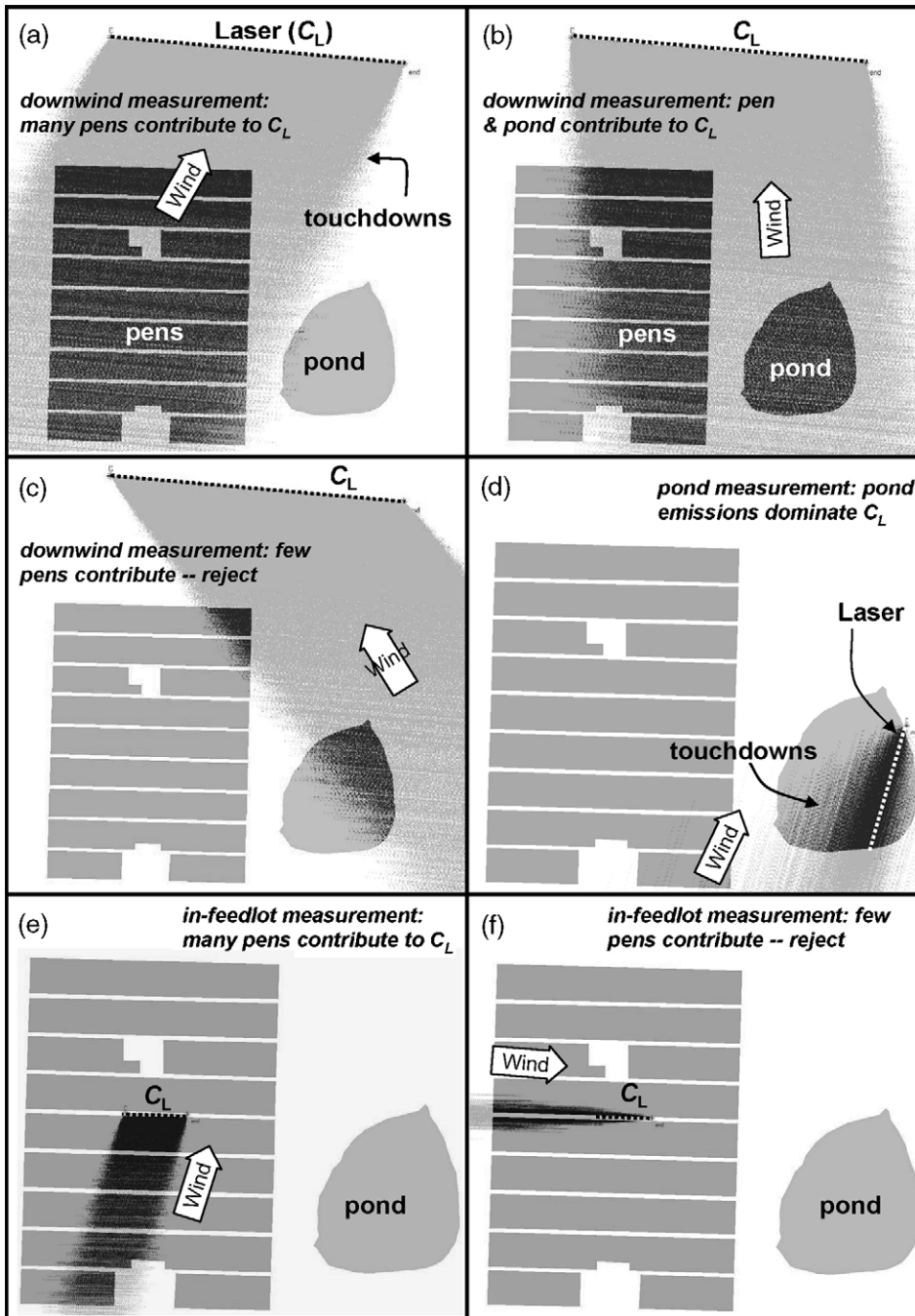


Fig. 4. Example bLS touchdown fields. These map the measurement footprint for a 15-min concentration measurement ( $C_L$ ), indicating where surface emissions influence  $C_L$ .

correlation with windspeed was expected given previous studies of  $\text{NH}_3$  emissions from nitrogen rich water surfaces (e.g., Denmead et al., 1982; Harper et al., 2000, 2006).

As we see in the following analysis,  $\text{NH}_3$  emission from the pond ( $\sim 200\text{--}300 \text{ kg day}^{-1}$ ) was a small

fraction of that from the pens (less than 5%). This is consistent with the typical runoff-pond emission estimates given by Koelsch and Stowell (2005). We therefore ignore the pond in our analysis. This allows us to calculate pen emissions even if the laser footprint extends into the pond (e.g., Fig. 4b).

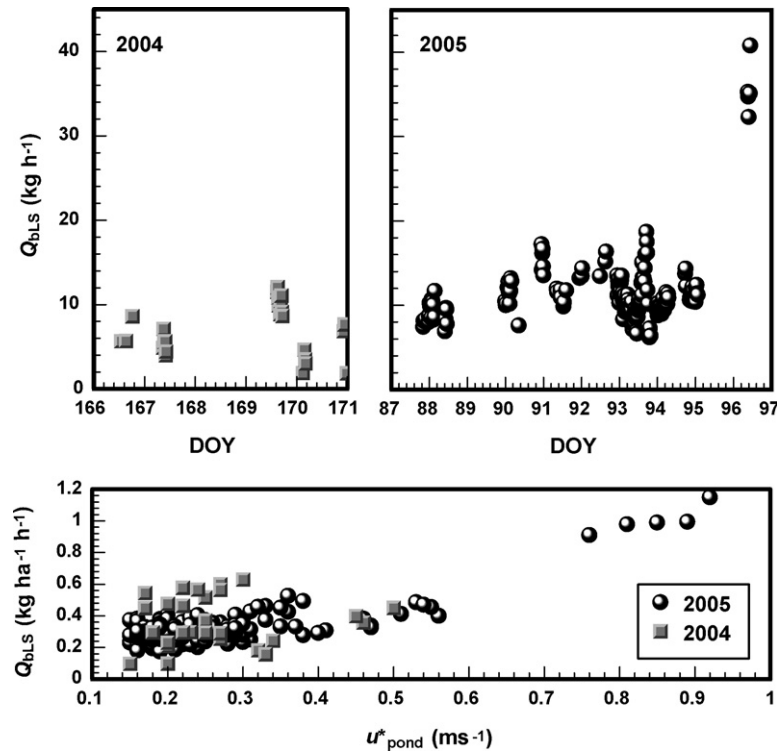


Fig. 5. Ammonia emissions from the runoff pond in 2004 and 2005. The top graphs show emissions plotted vs. day-of-year (DOY). The bottom graph shows the areal emission rate (per hectare) vs. the friction velocity measured over the pond ( $u^*_{\text{pond}}$ ).

## 5. Emissions from in-feedlot measurements

### 5.1. Advantage of in-feedlot location

Fig. 6 shows the  $C_L$  timeseries from the in-feedlot lasers. Measurements consist of 15-min averages, spanning 12 days (2004) and 10 days (2005). The data are not continuous, with gaps when the un-attended lasers became misaligned with the reflectors, or there was a loss of battery power. We observed high  $\text{NH}_3$  levels in the feedlot, with average concentrations of 1.7 ppm (2004) and 1.2 ppm (2005), and maximum values approaching 5 ppm in 2004. Because  $C_L$  is much higher than background levels, our bLS emission calculations are insensitive to uncertainties in  $C_b$ . This is not true for the downwind locations.

In-feedlot measurements also yield a much more complete emission timeseries than downwind observations. One reason for this is that emissions can be calculated from any wind direction, as the sensors are always in the feedlot plume. As well, the feedlot modifies the wind environment in a way that increases the usable data (i.e., provides for a more predictable wind regime). Fig. 7 shows 15-min wind statistics measured concurrently from the feedlot and ambient

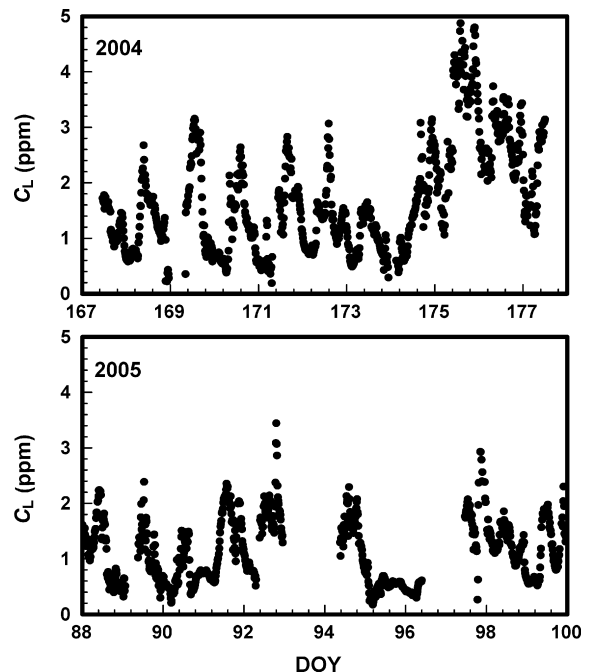


Fig. 6. Concentration ( $C_L$ ) timeseries plotted against day-of-year (DOY) for the in-feedlot lasers in 2004 (top) and 2005 (bottom). The measurement height was  $z_m = 1.2$  m (2004) and 1.0 m (2005).

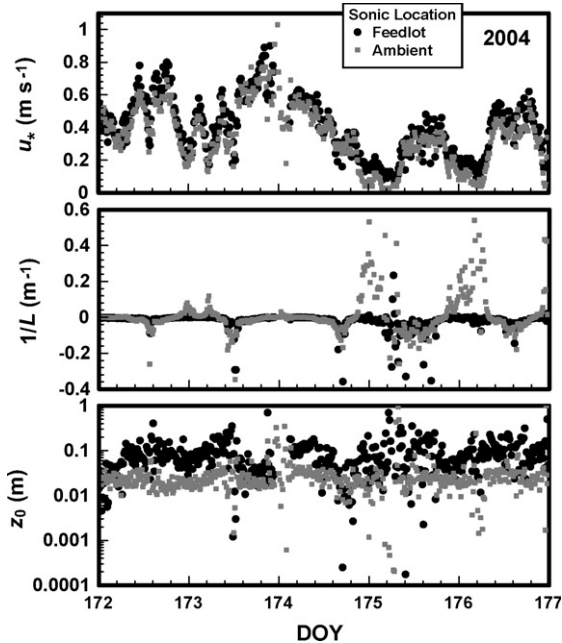


Fig. 7. Wind statistics measured/inferred from the feedlot and ambient sonic anemometers in 2004. Top graph shows the friction velocity  $u_*$ , the middle graph the reciprocal of the Obukhov stability length  $1/L$  (positive in stable stratification, negative in unstable), and the bottom graph shows the roughness length  $z_0$ .

sonics for several days in 2004. We see that the feedlot creates an internal boundary layer having a higher  $u_*$  (more wind shear) and a higher  $|L|$  (weaker thermal stratification) than in the ambient boundary layer, probably due to the increased roughness of the feedlot surface. Applying our filtering criteria (Section 3.3) to the ambient record in Fig. 7, we would reject 24% of observations because of low  $u_*$  and  $|L|$ . But for the feedlot wind record we would reject only 9% of these same observations.

## 5.2. Sensitivity to source configuration

A disadvantage of the in-feedlot location is sensitivity in  $Q_{\text{bLS}}$  to the assumed source configuration. While we assume  $\text{NH}_3$  emissions are uniform across the source, or non-uniform in some regular way, the actual emission sources (probably recent urine patches) are unevenly distributed: with infrequently populated loading areas, non-emitting roadways, uneven pen populations, etc. Here we consider how  $Q_{\text{bLS}}$  calculations are affected by the assumed configuration.

Fig. 8 illustrates four possible feedlots. The “solid” configuration takes the full pen outline as the source (excluding only an office area along the south edge). The “no-alley” configuration is similar, but excludes

the main alleys used by feeding trucks and a central loading area. In the “checkered” configuration we further eliminate minor pathways as sources, and assume 15% of the pens are empty (scattered randomly). The “feeding” configuration assumes emissions are concentrated in narrow bands along feeding troughs. We now compare  $Q_{\text{bLS}}$  calculations assuming these four configurations using our 2004 data.

Compared with the solid configuration, using the no-alley and checkered sources results in 16% larger feedlot emissions, while the feeding configuration gives 6% lower. These differences are explained by the source distribution immediately adjacent to the laser path, as the predicted  $(C_L/Q)_{\text{sim}}$  is most influenced by nearby emission sources. In the solid configuration the alley beneath the laser path is designated as “source”, while in the no-alley configuration it is not. The solid configuration thus requires a lower  $Q_{\text{bLS}}$  than the no-alley configuration in order to give the same  $C_L$ . In the feeding configuration the alley under the laser path is not a source, but source area is concentrated close by (i.e., along troughs adjacent to the alley) and this also results in lower emission calculation. Although the no-alley and checkered configurations are visually very different, the source distribution near the laser path is similar enough to give nearly identical  $Q_{\text{bLS}}$  results.

These calculations show the need to be attentive to source details near the laser path, but less concerned with distant details. We conclude it is important to use a configuration that recognizes the alleyway beneath the laser is not an emission source, and have thus chosen the “no-alley” configuration for our analysis. We also conclude that during feeding, which concentrates cattle near the feeding troughs, there may be a temporary bias in our emission calculations.

## 5.3. Average emission rates

Fig. 9 shows  $Q_{\text{bLS}}$  calculated from the in-feedlot  $C_L$  record. The most notable feature is the dramatic diurnal cycle in emissions. Maximum afternoon emissions approach  $1000 \text{ kg h}^{-1}$  on some days, with nighttime rates falling below  $100 \text{ kg h}^{-1}$ . If we calculate an ensemble average daily emission cycle (Fig. 10) we find 2004 and 2005 have a remarkably similar pattern, consistent with  $\text{NH}_3$  emissions closely tied to animal activity. We see a typical day having emissions at a minimum near  $100 \text{ kg h}^{-1}$  just before sunrise (6:00 LST). Thereafter emissions rapidly increase to  $400 \text{ kg h}^{-1}$  at 10:00 due to waking animals beginning to eat, drink, and urinate. There is an emission plateau from 10:00 until 12:00 that may correspond to less

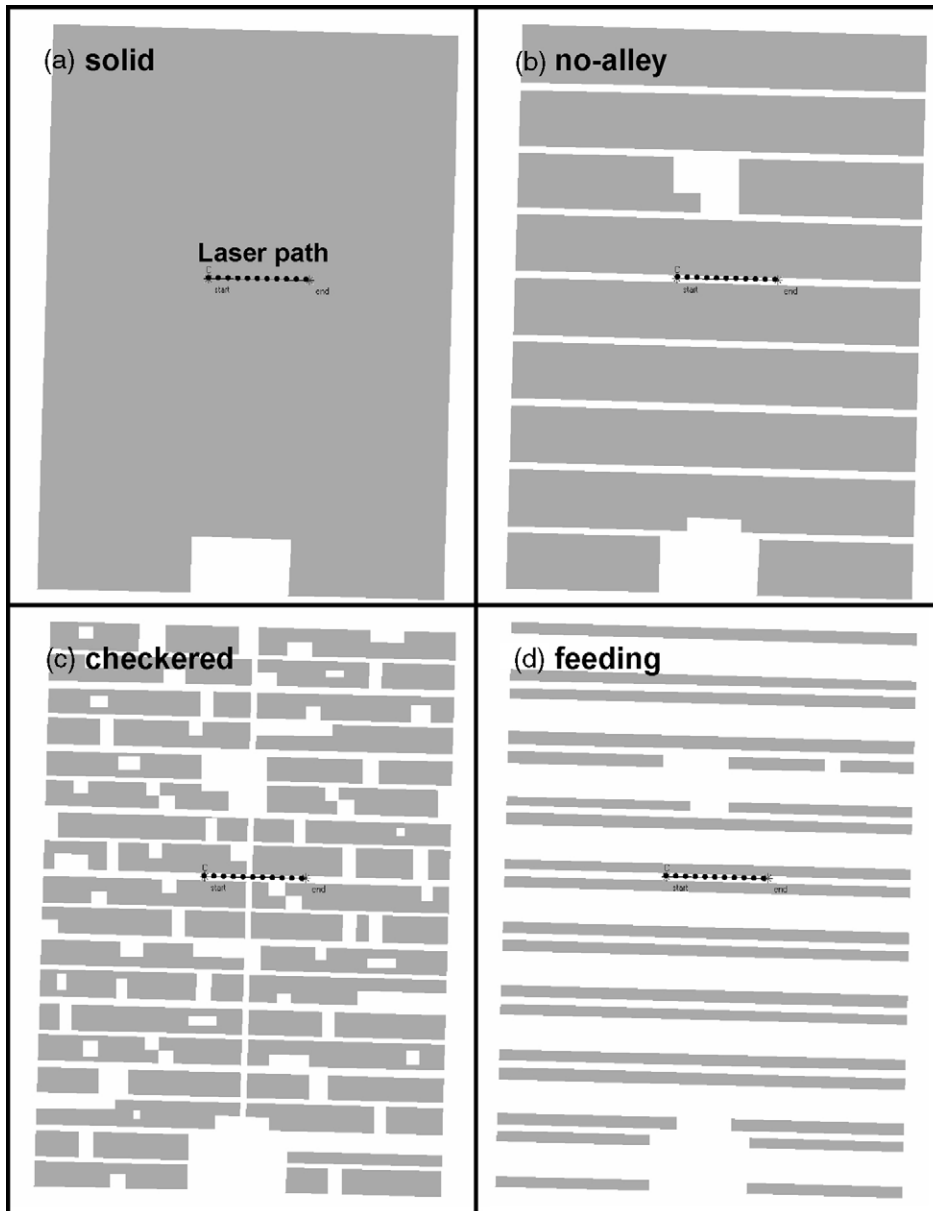


Fig. 8. Four feedlot configurations used in our bLS calculations.

active animals after feeding. Thereafter follows another period of increasing emissions, rising to an early afternoon maximum of  $500\text{--}600\text{ kg h}^{-1}$ . After this maximum there is a rapid decline in emissions until about 19:00 (sunset), after which is another plateau lasting about 1 h. We believe this corresponds to a burst of animal activity (visible to the observer) after sunset. A decline in emissions then lasts until the next sunrise. While there is some modulation of this cycle with windspeed and temperature (both positively correlated

with emissions), time-of-day seems the principle predictor of emissions. This close relationship between emissions and animal activity suggests that nitrogen in the cattle urine (the main source of  $\text{NH}_3$ ) is rapidly volatilized to  $\text{NH}_3$ .

From the daily emission cycle in Fig. 10 we calculate average feedlot emissions of  $Q_{\text{bLS}} = 7300\text{ kg day}^{-1}$  (2004) and  $6100\text{ kg day}^{-1}$  (2005). The 22% higher emission rate in 2004 can be interpreted as simply proportional to the 20% higher cattle population

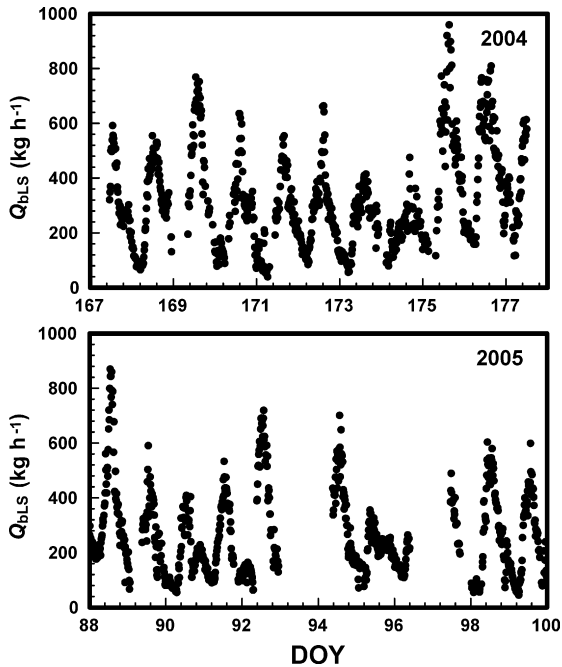


Fig. 9. Feedlot ammonia emissions  $Q_{bLS}$  plotted vs. day-of-year (DOY) for 2004 and 2005. Calculations are made using the in-feedlot measurements.

compared with 2005 (Table 1). It is interesting that higher 2004 emissions are not so much the result of uniformly higher emissions over the day, but a prolonged period of higher emissions into the late afternoon.

Fig. 11 shows how daily feedlot emissions vary during the experiment.<sup>7</sup> Most days are similar, with 12 of the 17 days having  $Q_{bLS}$  between 5000 and 7000 kg day<sup>-1</sup>. We see little evidence that daily emissions correlate with daily average air temperature or windspeed (Fig. 11). The most noticeable feature of the daily totals is the almost doubling of emissions during the last 2 days of the 2004 study.

#### 5.4. Comparison with other studies

The NH<sub>3</sub> emissions from the feedlot equates to 0.15 kg NH<sub>3</sub> animal<sup>-1</sup> day<sup>-1</sup> (Table 1), with remarkable consistency between the two study periods. This is considerably higher than the 0.05 kg animal<sup>-1</sup> day<sup>-1</sup>

<sup>7</sup> We include only days with at least 75% good  $Q_{bLS}$  observations. Missing data are estimated by linear interpolation. There are more complete days in 2004 by defining the day as noon-to-noon, while in 2005 we use midnight-to-midnight. For 3 days in 2004 where we lacked laser data, we used supplemental NH<sub>3</sub> concentrations taken at the in-feedlot tower (see Todd et al., 2005 for details).

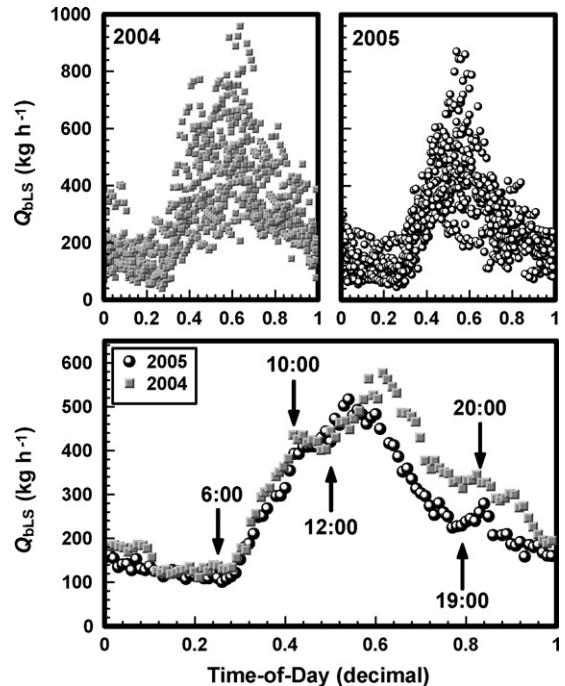


Fig. 10. Feedlot ammonia emissions  $Q_{bLS}$  plotted vs. decimal time-of-day (i.e., 0.5 = 12:00 LST) for 2004 (top left) and 2005 (top right). The bottom graph shows the ensemble average daily emissions. Emissions are calculated using in-feedlot measurements.

reported by Hutchinson et al. (1982) for a feedlot in Colorado. Our emissions were closer to values derived from Koelsch and Stowell (2005), who summarized emissions for typical animal production systems. Using their typical nitrogen (N) excretion value of 0.16 kg animal<sup>-1</sup> day<sup>-1</sup> (finishing cattle), and assuming 40–60% of the excreted N is lost by NH<sub>3</sub> volatilization (open-feedlot in hot arid region), gives emissions of 0.08–0.12 kg NH<sub>3</sub> animal<sup>-1</sup> day<sup>-1</sup>.

We also calculate the N lost in NH<sub>3</sub> emissions as a percentage of dietary N in the animal feed (Table 1). Our emissions correspond to 63% (2004) or 65% (2005) of the dietary N. A similar level of N efficiency is found in other studies. Bierman et al. (1999) calculated that, depending on feed composition, 51%, 59%, or 61% of the dietary N of feedlot steers was lost through volatilization in Nebraska. Erickson et al. (1999) calculated a 63% N loss for yearling cattle in Nebraska. And Todd et al. (2005) found 65% N loss in the same Texas feedlot used in this study, 1 year prior to our observations.

An interesting observation from our study is the dramatic increase in NH<sub>3</sub> emissions during the last 2 days in 2004 (Fig. 11). What explains this increase? In a feedlot situation Hutchinson et al. (1982) found NH<sub>3</sub>

Table 1  
Feedlot information for the two study periods

	Summer 2004	Spring 2005
No. of cattle	49,109	40,295
Daily feed (kg dry matter)	405,600	313,500
Daily N in feed <sup>a</sup> (kg)	9,470	7,760
Measurement period (days)	12	10
Daily emissions, $Q_{\text{bLS}}$ (kg NH <sub>3</sub> )	7,300	6,100
Daily emissions/head (kg NH <sub>3</sub> )	0.149	0.151
Daily emission density <sup>b</sup> (kg NH <sub>3</sub> /m <sup>2</sup> )	0.0094	0.0078
N loss from NH <sub>3</sub> volatilization, as percentage of dietary N input (%)	63	65

Cattle numbers and feed information are based on month averages. Pen emissions calculated from the in-feedlot measurements.

<sup>a</sup> Diet samples obtained immediately after feeding, with N determined after block digestion using a colorimetric procedure.

<sup>b</sup> Emission density is sensitive to the assumed source area. We use the “no-alley” configuration with a 78 ha source.

emissions were suppressed when the ground was wet, but enhanced as the surface then dried. We believe we see the same pattern. During the 24 h ending on Day 174, 13 mm of rain fell at the feedlot (Fig. 11). Emissions on this day and the following are among the lowest measured. But two days after the rain, when the surface had dried under sunny skies, we observed the dramatic increase in emissions.

## 6. Emissions from downwind measurements

### 6.1. Complications

Downwind laser measurements yield a much sparser record of emissions than the in-feedlot location. This is mostly due to the small range of useful wind directions that move the emission plume over the downwind laser

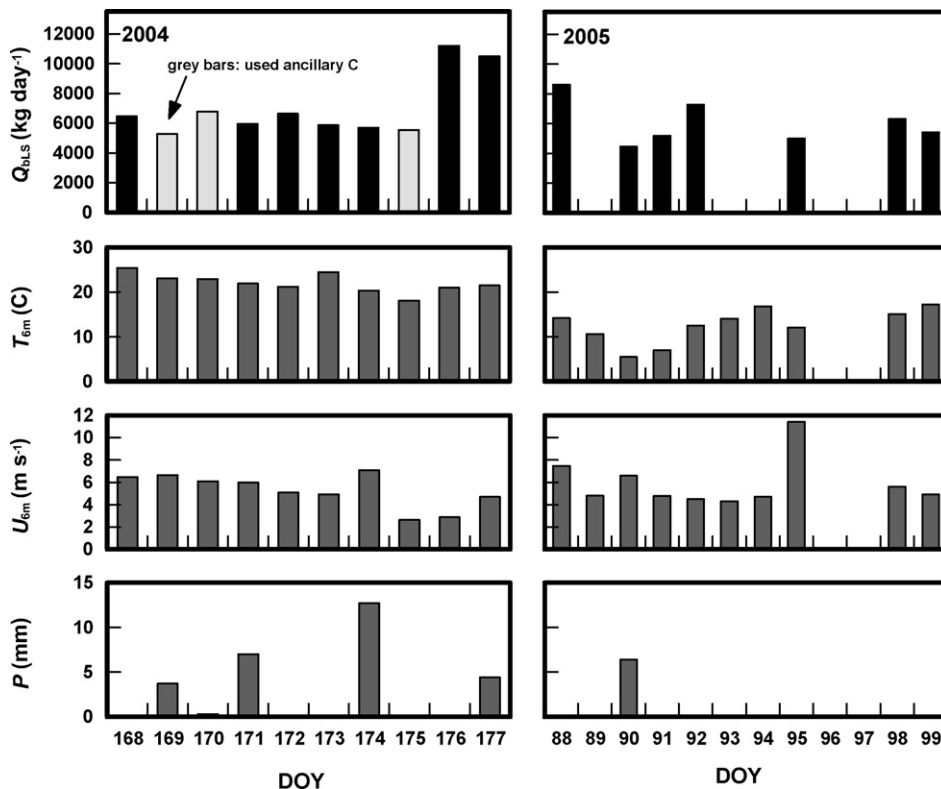


Fig. 11. Daily ammonia emissions ( $Q_{\text{bLS}}$ ), average in-feedlot air temperature at height  $z = 6$  m ( $T_{6\text{ m}}$ ), average in-feedlot windspeed at  $z = 6$  m ( $U_{6\text{ m}}$ ), and daily precipitation ( $P$ ) for 2004 (left graphs) and 2005 (right graphs). For 3 days in 2004 the  $Q_{\text{bLS}}$  are estimated with ancillary concentration measurements, indicated with light gray bars.

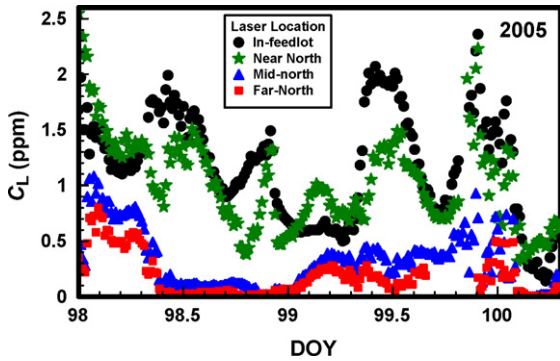


Fig. 12. Concentration ( $C_L$ ) timeseries, plotted vs. day-of-year (DOY), for the four lasers in 2005.

paths. The further downwind, the more this is a problem. For example, in 2005 there was a 70 h period when winds were generally from the south. Over this period we derive 47 h of emission data from the near-north laser, 26 h from the mid-north laser, and 23 h from the far-north laser (while the in-feedlot laser gives emission data for the entire period).

Fig. 12 shows  $\text{NH}_3$  concentrations from the lasers during this 2005 period. Concentrations at the near-north laser are alternately higher and lower than at the in-feedlot laser (for a due south wind we expect a maximum concentration at the near-north laser, but for other wind directions the concentration at the in-feedlot laser can be higher). At the mid- and far-north locations the concentrations are much lower, as one expects as gas is dispersed downwind. At times the concentration at these lasers is close to background levels. This adds considerable uncertainty to a diagnosis of emission rate, due to both poorer resolution of the lasers (as a percentage of  $C_L$ ) and the increased sensitivity to an uncertain  $C_b$ .

Another problem with a downwind location is the choice of wind statistics to use in the dispersion calculations. In Section 5.1 we discussed how the feedlot modifies the wind environment, creating an internal boundary layer characterized by a higher  $u_*$  and larger  $|L|$ . When we use downwind  $C_L$  to deduce  $Q_{\text{bLS}}$ , there are two choices for wind statistics, feedlot or ambient (this restriction stems from the fact that we instrumented only two locations). The best choice is not obvious.

## 6.2. Emission calculations from downwind lasers

In the following analysis we take  $Q_{\text{bLS}}$  calculated on the basis of the in-feedlot laser and sonic as

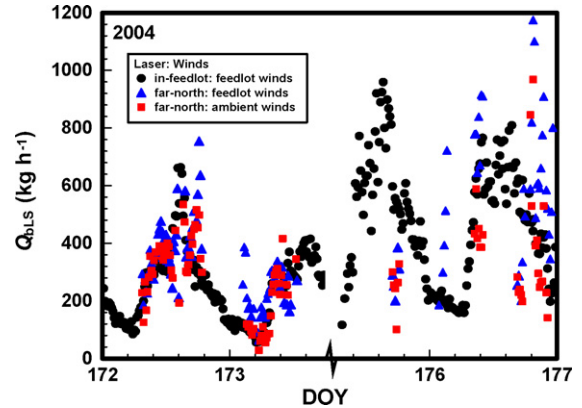


Fig. 13. Feedlot ammonia emissions ( $Q_{\text{bLS}}$ ) in 2004, plotted vs. day-of-year (DOY). Emissions were calculated from either the in-feedlot or far-north laser concentrations, and those calculated with the far-north laser use either the feedlot or ambient wind statistics.

“truth”, designated as  $Q$ . The ratios  $Q_{\text{bLS}}/Q$  from the downwind lasers ( $Q_{\text{near}}/Q$ ,  $Q_{\text{mid}}/Q$ ,  $Q_{\text{far}}/Q$ ) will then have an ideally accurate value of one. The average and standard deviation of these ratios are displayed in Table 2.

Fig. 13 shows  $Q_{\text{far}}$  calculated using the downwind laser<sup>8</sup> signal in 2004. There are several instances of good agreement between  $Q_{\text{far}}$  and  $Q$ , as during much of Days 172 and 173. But there are also periods of poor agreement, like the early evening of Day 176. The best overall results are obtained using wind statistics from the ambient sonic, which give an overall average  $Q_{\text{far}}/Q$  of 0.93 (with a standard deviation  $\sigma_{Q/Q} = 0.36$ ). Ratios using the feedlot wind statistics are inferior, with an average  $Q_{\text{far}}/Q$  of 1.40 ( $\sigma_{Q/Q} = 0.68$ ). The lower accuracy is mostly due to nighttime cases. From sunrise to sunset the use of the two alternative wind statistics (feedlot and ambient) yields similar levels of accuracy ( $Q_{\text{far}}/Q = 0.93, 1.14$ ).

In 2005 we see a similar situation to 2004, with periods of both good and poor results from the mid- and far downwind lasers (Fig. 14). The mornings of Days 98 and 99 are impressive periods, particularly when using the feedlot winds statistics in the bLS calculation. Using feedlot winds gives average ratios  $Q_{\text{mid}}/Q$ ,  $Q_{\text{far}}/Q$  that are a very good 1.13, 1.04 ( $\sigma_{Q/Q} = 0.44, 0.57$ ). Unlike 2004, the results using ambient winds are

<sup>8</sup> The two far-north lasers were positioned back-to-back (Fig. 2) in 2004. When both lasers were functioning we averaged  $C_L$  along their combined path and used this value to calculate  $Q_{\text{bLS}}$ . Otherwise only one laser was used.

Table 2

Average ratio of emissions calculated from three downwind lasers (near, mid, far) to that calculated with the feedlot laser/sonic ( $Q_{\text{near,mid,far}}/Q$ )

Dataset		$Q_{\text{near}}/Q$ wind statistics		$Q_{\text{mid}}/Q$ wind statistics		$Q_{\text{far}}/Q$ wind statistics	
		Ambient	Feedlot	Ambient	Feedlot	Ambient	Feedlot
All data	2004	–	–	–	–	0.93 (0.36)	1.40 (0.68)
	2005	0.75 (0.22)	1.09 (0.35)	0.70 (0.33)	1.13 (0.44)	0.61 (0.37)	1.04 (0.57)
Sunrise-to-sunset	2004	–	–	–	–	0.93 (0.37)	1.14 (0.45)
	2005	0.75 (0.19)	1.01 (0.28)	0.73 (0.28)	1.12 (0.49)	0.61 (0.36)	0.90 (0.63)

The standard deviation is given in parenthesis. Values are given for each year, using both the ambient and feedlot wind statistics (in 2004 only the far position was measured).

less accurate, with average  $Q_{\text{mid}}/Q$ ,  $Q_{\text{far}}/Q$  of 0.70, 0.61 ( $\sigma_{Q/Q} = 0.33, 0.37$ ).

The near-north laser in 2005 is a unique downwind location. Because it is so close to the feedlot, the choice to use feedlot wind statistics in the bLS calculations is obvious: the transport of  $\text{NH}_3$  “seen” by the laser occurs almost exclusively in the feedlot boundary layer. This explains why our best downwind results are from the near-north  $C_L$  combined with the feedlot wind statistics. The average ratio  $Q_{\text{near}}/Q$  is a very good 1.09 ( $\sigma_{Q/Q} = 0.35$ ), and for daytime cases (sunrise-to-sunset)

the agreement is even better, with  $Q_{\text{near}}/Q = 1.01$  ( $\sigma_{Q/Q} = 0.28$ ).

### 6.3. Sources of uncertainty

The accuracy of our calculations using downwind concentrations can be interpreted as reasonably good: on average we were within 15% of the “true” emissions when using ambient wind statistics in 2004, and feedlot wind statistics in 2005. Considering  $Q_{\text{bLS}}$  from the different lasers corresponds to emissions from different areas of the feedlot, some differences are to be expected. But other of our downwind calculations are not so accurate, and the pattern of calculated emissions is confusing, e.g., why the better results using ambient wind statistics in 2004, but feedlot wind statistics in 2005? Some of this confusion is likely due to problems inherent in any downwind inference (e.g., low concentrations, sensitivity to wind measurement error). We believe, however, that two fundamental factors confound our results: inhomogeneity of the wind statistics, and dry deposition.

#### 6.3.1. Wind complexity

Ambiguity in deducing feedlot emissions from downwind concentration is anticipated when the ambient and feedlot wind regimes are very different, as this inevitably means a complex wind regime downwind of the feedlot, and potential inaccuracy in our simple dispersion model. We expect this at night. As the ambient atmosphere becomes stably stratified after sunset (i.e., suppressing the turbulence), the feedlot boundary layer tends to remain in a near-neutral or even unstable state. As a group the least accurate calculations occur at night, particularly when the ambient  $u_*$  and  $|L|$  fall below our threshold criteria, but the feedlot values do not. In these cases, with  $Q_{\text{bLS}}$  calculated from downwind concentrations and feedlot winds, the average  $Q_{\text{far}}/Q$  is a poor 1.87 (2004) and 1.27 (2005).

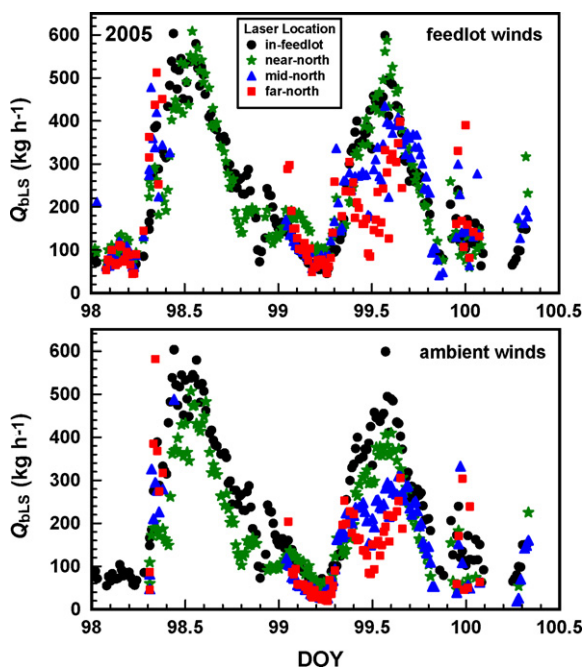


Fig. 14. Feedlot ammonia emissions  $Q_{\text{bLS}}$ , plotted vs. day-of-year (DOY), using the in-feedlot and north lasers in 2005. In the top graph the feedlot wind statistics are used in the calculations. In the bottom graph the ambient wind statistics are used (except with the in-feedlot laser).

### 6.3.2. Dry deposition

In 2005 we observe periods when  $Q_{\text{bLS}}$  calculated using downwind concentrations lies well below  $Q$ , no matter if feedlot or ambient wind statistics are used. Such a pattern of suppressed  $Q_{\text{bLS}}$  would occur if  $\text{NH}_3$  is removed from the atmosphere downwind of the feedlot: the reduction in  $C_L$  would be attributed to a reduction in  $Q_{\text{bLS}}$ . Surface deposition and chemical transformation are two possible removal processes. Although we assume  $\text{NH}_3$  to be a passive tracer in our calculations, it can be very reactive (Harper, 2005). Asman and van Jaarsveld (1992) simulated ammonia transport downwind of a surface point source in northern European conditions, and predicted that 20% of the emitted  $\text{NH}_3$  would be deposited (or absorbed) on the plant/ground surface within 1 km of the source (they also calculated the transformation of  $\text{NH}_3$  to  $\text{NH}_4^+$  was important, but at longer ranges than our situation). Among other factors,  $\text{NH}_3$  deposition depends on surface characteristics (Harper and Sharpe, 1998): e.g., a well-watered crop (producing open stomates), higher windspeeds (to transport  $\text{NH}_3$  into the plant canopy), and higher solar radiation (higher rate of photosynthesis) promote  $\text{NH}_3$  absorption.

A suspicion that deposition occurs is created when pondering the inferred emission pattern on Day 99 in 2005 (Fig. 14). During mid-morning (e.g., DOY = 99.3–99.4) we see good accuracy from the downwind lasers. But after 9:30 LST  $Q_{\text{mid}}$  and  $Q_{\text{far}}$  decline, even as  $Q$  increases. Near noon  $Q_{\text{far}}$  is roughly 50% of  $Q$ . Thereafter  $Q_{\text{mid}}$  and  $Q_{\text{far}}$  rise to match again the actual emissions by late afternoon. This trend –  $Q_{\text{bLS}}$  suppression beginning about 9:30, peaking at 12:00, and ending at 16:00 – follows our expectation for the timing of stomatal opening and closing, and maximum photosynthesis (and consequent utilization of atmospheric  $\text{NH}_3$ ). The fact that “suppression” of  $Q_{\text{bLS}}$  increases with measurement distance (Fig. 14) is further evidence that deposition is occurring, since more  $\text{NH}_3$  would be removed as distance increases. We note the spring of 2005 had above-average precipitation, and our early April observations coincided with rapid growth of vegetation in the pasture north of the feedlot—factors promoting deposition. The limited afternoon data we have in 2004 (Days 172, 173, 175, and 176) also shows a  $Q_{\text{far}}$  reduction compared to  $Q$ , and to about the same degree as on Day 99 in 2005.

We believe the surface deposition of  $\text{NH}_3$  at our site results in errors in the emission calculations using downwind concentrations. Although we identify a probable deposition “signal” during the daytime, there may be deposition at other times as well. If dew forms at

night, for example, the plant and soil surface will be a strong sink for  $\text{NH}_3$  (e.g., Harper et al., 1987). There may then be  $\text{NH}_3$  re-emission as the dew evaporates, further confounding an emission inference. These phenomena indicate the danger of using downwind measurement locations for reactive gases like ammonia.

## 7. Summary and conclusions

We demonstrated the application of a bLS inverse-dispersion technique to estimate bulk  $\text{NH}_3$  emissions from a beef-cattle feedlot. This technique neglects the non-uniformity of the boundary layer over the feedlot and uses a simple bLS dispersion model to relate observed  $\text{NH}_3$  concentrations to the emission rate  $Q_{\text{bLS}}$ . While the assumption of idealized winds is incorrect, we argue that these simplifications are acceptable for carefully selected measurement locations.

We considered two categorically different measurement locations: within the feedlot and downwind. The in-feedlot location was superior, having the advantage that:

- Emission rates could be calculated for almost all wind directions.
- Higher  $\text{NH}_3$  concentrations reduce measurement uncertainty and sensitivity to an unknown background concentration.
- Because this was a large feedlot, one could be confident that a sonic anemometer positioned in the feedlot interior would provide representative wind statistics ( $u^*$ ,  $L$ ,  $z_0$ ,  $\beta$ ) for the dispersion calculations.
- Aerodynamic characteristics of the feedlot act to create a more strongly sheared (higher  $u^*$ ) and less stratified (higher  $|L|$ ) flow than outside the feedlot, increasing the number of useable observations.

Using in-feedlot measurements, we found average emissions of  $0.15 \text{ kg NH}_3 \text{ animal}^{-1} \text{ day}^{-1}$  in both 2004 and 2005. This represents a loss of 63% (2004) or 65% (2005) of the dietary N. We view the agreement between our observations and other studies, and the self-consistency of our measurements (between years and between measurement locations), as confirmation of the accuracy of bLS—provided it is applied carefully in light of the factors exposed in detail above.

A downwind measurement location also provided good  $Q_{\text{bLS}}$  estimates, however, several difficulties were encountered:

- Only a narrow range of wind directions allowed a good  $Q_{\text{bLS}}$  estimate.

- Lower  $\text{NH}_3$  concentrations increased measurement uncertainty and sensitivity to the unknown background concentration.
- Uncertainty in whether to use ambient or feedlot wind statistics in calculations.
- Surface deposition of  $\text{NH}_3$  probably caused errors in the emission calculations.

For the most distant concentration measurement (approximately 600 m from the feedlot) we saw that, for a combination of different years (2004 and 2005) and different wind statistics (feedlot, ambient), the calculated emissions were 93%, 61%, 126%, and 110% of that determined from in-feedlot measurements.

The idealized bLS technique demonstrated at our feedlot should be applicable to similar situations where a large emission source modifies the ambient winds. Our recommendation is to use in-source concentrations and wind measurements in the calculation (although avoiding locations near the upwind edge of the source). If downwind measurements are necessary, we suggest a location as close to the source as possible, using in-source or near-source wind statistics in the dispersion calculations.

This recommendation appears to conflict with those given by Flesch et al. (2005a,b) and McGinn et al. (2006). When dealing with sources associated with localized wind disturbances, they suggest the best strategy is to move downwind. However, this applies for cases where there is a prompt return to ambient conditions a short distance downwind. For our large feedlot, this distance would be very large. Evidently then, the horizontal scale of the source disturbance ( $x_{\text{src}}$ ) is an important factor for deciding on measurement locations. For a large source one must go far downwind to a location where the ambient winds are the appropriate choice for an idealized bLS calculation, and this distance will scale on  $x_{\text{src}}$  (and not the height of the wind obstacles as in the example of Flesch et al. (2005a,b)). However, for sources with a large  $x_{\text{src}}$  like our feedlot, the better choice is probably to use in-source or near-source measurement locations.

### Acknowledgements

This work has been supported by research grants from the Natural Sciences and Engineering Research Council of Canada (NSERC) and the Canadian Foundation for Climate and Atmospheric Sciences (CFCAS). Financial support has also been provided by the United States Department of Agriculture (Cooperative State Research, Education, and Extension

Service; the Agricultural Research Service). The authors would also like to acknowledge the technical support of J. Scarbrough, M. Thornton, L. McDonald, H. Perkins, and A. Mason.

### References

- Asman, W.A.H., van Jaarsveld, J.A., 1992. A variable-resolution transport model applied for  $\text{NH}_x$  for Europe. *Atmos. Environ.* 26A, 445–464.
- Bierman, S., Erickson, G.E., Klopfenstein, T.J., Stock, R.A., Shain, D.H., 1999. Evaluation of nitrogen and organic matter balance in the feedlot as affected by level and source of dietary fiber. *J. Anim. Sci.* 77, 1645–1653.
- Boadi, D.A., Wittenberg, K.M., Scott, S.L., Burton, D., Buckley, K., Small, J.A., Ominski, K.H., 2004. Effect of low and high forage diet on enteric and manure pack greenhouse gas emissions from a feedlot. *Can. J. Anim. Sci.* 84, 445–453.
- Denmead, O.T., Freney, J.R., Simpson, J.R., 1982. Dynamics of ammonia volatilization during furrow irrigation of maize. *Soil Sci. Soc. Am. J.* 46, 149–155.
- Denmead, O.T., Raupach, M.R., 1993. Methods for measuring atmospheric gas transport in agricultural and forest systems. In: *Agricultural Ecosystem Effects on Trace Gases and Global Climate Change*, .
- Dyer, A.J., 1974. A review of flux-profile relationships. *Bound. Layer Meteor.* 7, 363–372.
- Erickson, G., Klopfenstein, T., Milton, T., Herold, D., 1999. Effects of Matching Protein to Requirements on performance and Waste Management in the Feedlot. University of Nebraska Cooperative (Extension MP 71).
- Farran, T.B., Erickson, G.E., Klopfenstein, T.J., Macken, C.N., Lindquist, R.U., 2006. Wet corn gluten feed and alfalfa hay levels in dry-rolled corn finishing diets: effects on finishing performance and feedlot nitrogen mass balance. *J. Anim. Sci.* 84, 1205–1214.
- Flesch, T.K., Wilson, J.D., 2005. Estimating tracer emissions with a backward Lagrangian stochastic technique. In: Hatfield, J.L., Baker, J.M. (Eds.), *Micrometeorology in Agricultural Systems*. American Society of Agronomy, Madison, WI, pp. 513–531.
- Flesch, T.K., Wilson, J.D., Harper, L.A., 2005a. Deducing ground-air emissions from observed trace gas concentrations: a field trial with wind disturbance. *J. Appl. Meteorol.* 44, 475–484.
- Flesch, T.K., Wilson, J.D., Harper, L.A., Crenna, B.P., 2005b. Estimating gas emission from a farm using an inverse-dispersion technique. *Atmos. Environ.* 39, 4863–4874.
- Flesch, T.K., Wilson, J.D., Harper, L.A., Crenna, B.P., Sharpe, R.R., 2004. Deducing ground-air emissions from observed trace gas concentrations: a field trial. *J. Appl. Meteorol.* 43, 487–502.
- Garratt, J.R., 1992. *The Atmospheric Boundary Layer*. Cambridge University Press, New York, 316 pp.
- Harper, L.A., 2005. Ammonia: Measurement Issues. In: Hatfield, J.L., Baker, J.M. (Eds.), *Micrometeorological measurements in agricultural systems*. Agron. Monogr. 47. ASA, CSSA, and SSSA, Madison WI, pp. 345–379.
- Harper, L.A., Sharpe, R.R., 1998. Atmospheric ammonia: issues on transport and nitrogen isotope measurement. *Atmos. Environ.* 32, 273–277.
- Harper, L.A., Sharpe, R.R., Langdale, G.W., Giddens, J.E., 1987. Nitrogen cycling in a wheat crop: soil, plant, and aerial nitrogen transport. *Agron. J.* 79, 965–973.

- Harper, L.A., Sharpe, R.R., Parkin, T.B., 2000. Gaseous emissions from anaerobic swine lagoons: ammonia, nitrous oxide, and dinitrogen gas. *J. Environ. Qual.* 29, 1356–1365.
- Harper, L.A., Weaver, K.H., Dotson, R.A., 2006. Ammonia emissions from swine waste lagoons in the Utah Great Basin. *J. Environ. Qual.* 35, 224–230.
- Hutchinson, G.L., Mosier, A.R., Andre, C.E., 1982. Ammonia and amine emissions from a large cattle feedlot. *J. Environ. Qual.* 11, 288–293.
- Kaharabata, S.K., Schuepp, P.H., Desjardins, R.L., 2000. Source strength determination of a tracer gas using an approximate solution to the advection-diffusion equation for microplots. *Atmos. Environ.* 34, 2343–2350.
- Kaimal, J.C., Finnigan, J.J., 1994. *Atmospheric Boundary Layer Flows*. Oxford Univ. Press, 289 pp.
- Kaimal, J.C., Gaynor, J.E., 1991. Another look at sonic thermometry. *Bound. Layer Meteorol.* 56, 401–410.
- Koelsch, R., Stowell, R., 2005. Ammonia Emissions Estimator. University of Nebraska Extension, Lincoln, NE. <http://cnmp.unl.edu/AmmoniaEmissionsEstimator-21805.pdf>.
- McGinn, S.M., Flesch, T.K., Harper, L.A., Beauchemin, K.A., 2006. An approach for measuring methane emissions from whole farms. *J. Environ. Qual.* 35, 14–20.
- Paulson, C.A., 1970. The mathematical representation of wind speed and temperature profiles in the unstable atmospheric surface layer. *J. Appl. Meteor.* 9, 857–861.
- Todd, R.W., Cole, N.A., Harper, L.A., Flesch, T.K., Baek, B.H., 2005. Ammonia and gaseous nitrogen from a commercial beef cattle feedyard estimated using the flux-gradient method and N:P ratio analysis. In: *Proceedings of the Symposium on State of Science: Animal and Waste Management*, San Antonio, TX.
- Wilson, J.D., Flesch, T.K., Harper, L.A., 2001. Micro-meteorological methods for estimating surface exchange with a disturbed wind-flow. *Agric. For. Meteorol.* 107, 207–225.